Molecular Crystals and Liquid Crystals

Publication details, including instructions for authors and subscription information:
http://www.tandfonline.com/loi/gmcl20

Development of Experimental Methods for Determining the Electronic Structure of Organic Materials

Kazuhiko Seki [a] & Kaname Kanai [b]

[a] Research Center for Materials Science and Institute for Advanced Research, Nagoya University, Furo-cho, Chikusa-ku, Nagoya, Japan

[b] Department of Chemistry, Graduate School of Science, Nagoya University, Furo-cho, Chikusa-ku, Nagoya, Japan

Version of record first published: 31 Jan 2007

To cite this article: Kazuhiko Seki & Kaname Kanai (2006): Development of Experimental Methods for Determining the Electronic Structure of Organic Materials, Molecular Crystals and Liquid Crystals, 455:1, 145-181

To link to this article: http://dx.doi.org/10.1080/15421400600803713

Mol. Cryst. Liq. Cryst., Vol. 455, pp. 145–181, 2006

ISSN: 1542-1406 print/1563-5287 online
DOI: 10.1080/15421400600803713

Taylor & Francis
Taylor & Francis Group

Development of Experimental Methods for Determining the Electronic Structure of Organic Materials

Kazuhiko Seki
Research Center for Materials Science and Institute for Advanced Research, Nagoya University, Furo-cho, Chikusa-ku, Nagoya, Japan

Kaname Kanai
Department of Chemistry, Graduate School of Science, Nagoya University, Furo-cho, Chikusa-ku, Nagoya, Japan

The principles and developments of experimental methods for determining the energy parameters governing the electronic structure of organic molecules and solids are reviewed with some historical descriptions. The energy parameters discussed are ionization energy of a molecule (I_g) and solid (I_s), electron affinity of a molecule (A_g) and solid (A_s), and the energies of the vacuum level (VL) and the Fermi level (E_F). The work function (Φ) can be also derived as the difference between the last two. Various types of spectroscopic and electrical measurements are discussed with typical examples, including the range of applicability and the merits and the demerits. Recent microscopic techniques for obtaining local information are also described.

Keywords: band bending; dipole layer; doping; electronic structure; interface; photoelectron spectroscopy

One of the authors (K. S.) thanks Professor Hiroo Inokuchi for introducing him into the exciting scientific field organic semiconductors and conductors and for the constant encouragement and stimulation. This work was supported in part by the Grant in Aid for Creative Scientific Research "Elucidation and Control of Interfaces Related to Organic Electronic Devices" from the Japan Society for the Promotion of Science and the 21st COE Program "Establishment of COE on Materials Science: Elucidation and Creation of Molecular Functions" from the Ministry of Education, Culture, Science, Sports, and Technology of Japan.

Address correspondence to Kazuhiko Seki, Research Center for Materials Science and Institute for Advanced Research, Nagoya University, Furo-cho, Chikusa-ku, Nagoya 464-8602, Japan. E-mail: seki@mat.chem.nagoya-u.ac.jp

INTRODUCTION

Since the early days of the research on organic semiconductors and conductors, the determination of their electronic structure formed the basis for understanding and controlling their electronic and electrical properties. The electronic structure can be regarded as a theater in which electrons and holes play various roles as actors/actresses. Thus various techniques have been developed for determining their electronic structures of the organic materials. Most of them are various spectroscopic methods, but some are also based on electrical measurements. Also we note that many of the methods are more or less surface sensitive, and care is necessary to discriminate the contribution from the bulk and the surface. Although the early techniques probed the average of the energy parameters over a macroscopic area, more local information has also become available thanks for the recent progress of microscopic techniques. Recent development of organic thin film electronics also triggered the interest in the electronic structure of the organic/metal, organic/organic, and other interfaces, and they are also studies by similar experimental techniques.

In this article, we will briefly look back the development of these methods and discuss their principles and examples. We note that earlier articles are available for the history by 1980s about the methods for examining ionization energy [1] and electron affinity [2] in this journal, which were written at similar occasion of commemorating the 40 years of organic semiconductors. Also we note that most discussion and the experimental data were taken from molecular solids. A brief mention will be also made for polymers at the end of the article. We apologize in advance that our historical survey including the coverage of methods may not be very complete, and appreciate the notice of such cases to the authors.

ELECTRONIC STRUCTURE OF ORGANIC MOLECULE AND MOLECULAR SOLID

In Figure 1, we schematically depict the electronic structure of an organic solid with that of an isolated constituent molecule, with several leading energy parameters. In a molecule (see Fig. 1(a)), many electronic energy levels are formed in the potential well formed by atomic nuclei and other electrons. The core levels are isolated in the deep well formed by each nucleus, while valence levels are delocalized over the molecule, forming the *molecular orbitals* (MOs). The edge of the potential well corresponds to the energy of a rest electron just outside of the molecule, and is called *vacuum level* (VL). The energies of

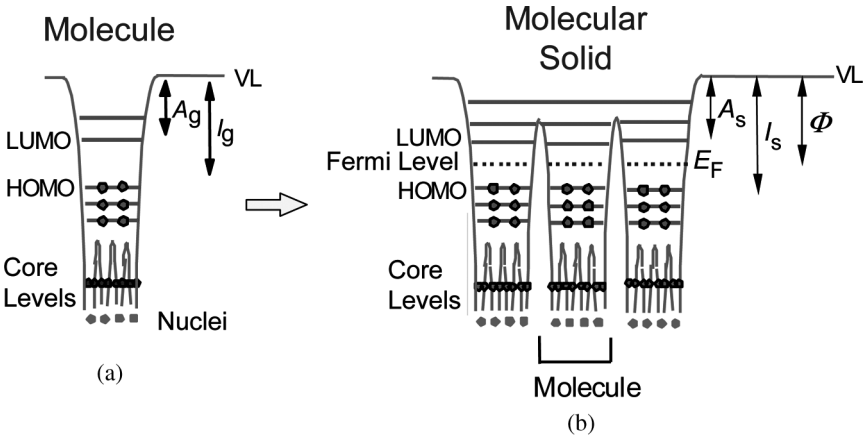

FIGURE 1 The electronic structures of (a) an isolated molecule and (b) a molecular solid formed by the aggregation of molecules. The energy parameters are I_g: gas phase ionization energy, A_g: gas phase electron affinity, I_s: solid state ionization energy, A_s: solid state electron affinity, and Φ: work function. VL denotes the energy of vacuum level just outside of the system, and E_F is the Fermi level.

the highest occupied MO (HOMO) ε(HOMO) and the lowest unoccupied MO (LUMO) ε(LUMO) correspond to the *gas phase ionization energy* (I_g) and the *gas phase electron affinity* (A_g) of a molecule, respectively, with relations

$$I_g = -\varepsilon(\text{HOMO}), \tag{1}$$

$$A_g = -\varepsilon(\text{LUMO}), \tag{2}$$

where g stands for the gas phase. The relations (1) and (2) are known as the Koopmans' theorem [3], and applies to the orbital energies calculated by Hartree-Fock calculations.

In an organic solid (see Fig. 1(b)), the molecules are usually bound by weak van der Waals interaction. Thus the electronic structure of a molecule is mostly preserved in the potential well of a molecule, although the finite overlap of the wavefunctions of the HOMO and LUMO leads to some electrical conduction by the move of holes or electrons, respectively. These states can be called the *valence* and *conduction bands* in the term of band theory, although the validity of the band theory based on the concept of itinerant carriers in states delocalized over the solid has to be examined in individual case [4].

The energetics of career formation can be discussed using two leading parameters: *solid state ionization energy* (I_s) and *solid state*

TABLE 1 Methods for Determining the Energy Parameters of Molecules and Molecular Solids

Energy parameter or level	Symbol	Method	Abbreviation	Note
Gas Phase Ionization Energy	I_g	Rydberg Series		
		Electron Impact Mass Spectrometry	EI	
		Photoionization Yield Spectroscopy	PYS	
		UV Photoelectron Spectroscopy	UPS	
		(Oxidation Potential)		Indirect method
		(Charge-transfer Spectrum)		Indirect method
Gas Phase Electron Affinity	A_g	Magnetron	MT	For $A_g > 0.8$ eV
		Electron Capture Detector	ECD	$0.1 < A_g < 0.9$ eV
		Alkali Metal Beam	AMB	
		Thermal Charge Transfer	TCT	
		Electron Transmission Spectroscopy	ETS	For Å $A_g < 0$
		Photodetachment Spectroscopy	PDS	For Å $A_g > 0$
		(Reduction potential)		Indirect method
		(Charge-transfer Spectrum)		Indirect method
		[Near-edge X-ray Absorption Fine Structure Spectroscopy][b]	NEXAFS	Often misleading
		[Electron Energy Loss Spectroscopy]	EELS	Often misleading

Solid State Ionization Energy	I_s	Photoemission Yield Spectroscopy	PYS	
		Millikan Appartus		
		UV Photoelectron Spectroscopy	UPS	
		Metastable Atom Electron Spectroscopy	MAES	
		Two Photon Photoemission Spectroscopy	2PPE	
		Internal Photoemission		
		Photoelectron Microscopy		
		Scanning Tunneling Microscopy	STS	
Solid State Electron Affinity	A_s	Internal Photoemission		
		Electron Transmission Spectroscopy	ETS	
		Inverse Photoemission Spectroscopy	IPES	
		Two Photon Photoemission Spectroscopy	2PPE	
		Photodetachment Spectroscopy of Clusters	PDS	
		[Near-edge X-ray Absorption Fine Structure Spectroscopy]	NEXAFS	Often misleading
		[Electron Energy Loss Spectroscopy]	EELS	Often misleading
		Scanning Tunneling Microscopy	STS	
		Ballistic Electron Emission Spectroscopy	BEEM	
Vacuum Level	VL	UV Photoelectron Spectroscopy	UPS	
		Photoelectron Microscopy		
		Kelvin Probe	KP	
		Kelvin Force Microscopy	KFM	
Fermi Level	E_F	UV Photoelectron Spectroscopy	UPS	
		Inverse Photoemission Spectroscopy	IPES	
		Kelvin Probe	KP	

electron affinity (A_s). The energies of *Fermi level* (E_F) and VL are also used for discussing the energetics in organic solids. E_F corresponds to the chemical potential of an electron in the solid, and often dominates the possible band bending at the interface. The location of the Fermi level may move within the *bandgap* (E_g) between the HOMO and the LUMO, depending on the various types of intentional and unintentional doping. The energy of VL in Figure 1(b) is the energy of a rest electron just outside of the solid. The energy difference between E_F and VL is called *work function* (Φ), which is also an important energy parameter.

In the following, we will discuss the methods used for determining these energy parameters, including their principles, typical examples, and some historical notes about their development. We focus our attention mostly on direct methods for determining these parameters, although we make a brief mention to indirect methods. In Table 1, we summarize their names, information obtained, and some notes.

ENERGY PARAMETERS OF ISOLATED MOLECULE

As seen in Figure 1(a), two leading energy parameters for an isolated organic molecule are gas phase ionization energy (I_g) and electron affinity (A_g). The molecules with small I_g and large A_g are known as *electron donors* and *acceptors*, respectively. These parameters show fairly wide range of variation (e.g., I_g from 4.4 eV for decamethylnickellocene [5] to 15.3 eV for SF_6 [6] and A_g from -1.15 eV for benzene [7] to 2.80 eV for tetracyanoquinodimethane TCNQ [8]). Also we can manipulate these quantities by proper design of the molecular structure, e.g., the construction of an appropriate conjugated system and introduction of various substituents. At the moment, probably the most comprehensive source of the values of I_g and A_g is the website of NIST Chemistry WebBook [9].

In discussing these quantities, we should note the distinction between the *adiabatic* and *vertical* values obtained at the experiments. The adiabatic value corresponds to the energy difference between the neutral and ionized species at their equilibrium geometries. Usually methods examining the thermal equilibrium give this value. In many optical spectroscopies, on the other hand, the peak in the spectrum corresponds to a transition *without* the change of molecular geometry, which is called vertical transition. Thus the obtained energy of the peak corresponds to the energy difference at the stable geometry of the starting species. The difference between the two types of values can be large when the removed/attached electron occupies

bonding or antibonding MO, where the ionization can lead to large change of equilibrium geometry.

In the following, we will describe the methods used for determining the values of I_g and A_g.

1. Gas Phase Ionization Energy (I_g)

The values of I_g have been studied by various methods from early period of 1930s by observing electron emission or closely related phenomenon such as the analysis of the Rydberg series and the electron impact (EI) mass spectrometry. The results obtained formed the earliest set of data among the energy parameters discussed here, and served as the basis for examining various molecular processes. This was followed by more precise values obtained by photoionization yield spectroscopy (PYS) in 1950s, and the development of UV photoelectron spectroscopy (UPS) from the latter half of 1960s further extended the study to the whole valence occupied states. The principles of these techniques are schematically illustrated in Figure 2.

(a) Rydberg Series in the Electronic Absorption Spectrum [10,11]

The value of I_g is determined from a series of high-energy optical transitions converging to I_g (see Fig. 2(a)). These transitions, called *Rydberg series*, correspond to the electron excitations from the HOMO to high energy orbitals with large radii, in which the excited electron rotates around the left of the molecule, which is similar with a molecular cation with a positive charge due to the hole in the HOMO. Thus these states are like excited hydrogen atom with heavy nucleus, and the transitions can be analyzed as such. If the spectral assignments and the analysis are properly carried out, the accuracy of the obtained ionization energy is high [11]. In Figure 3(a), an example for benzene is shown, with assigned transitions converging to the ionization energies of the 4 uppermost occupied MOs indicated by the hatched bars [12]. Unfortunately, however, many large organic molecules do not show clear series of absorption.

(b) Electron Impact (EI) Mass Spectrometry

In this method, molecular cation formation at electron impact is studied by mass spectrometry as a function of incident electron energy E_i [13]. The value of I_g is determined as the minimum E_i for the cation formation (see Fig. 2(b)). The accuracy is often not so high due to the slow rise at the onset and the complexity due to possible molecular fragmentation. Although the method can be in principle applied to

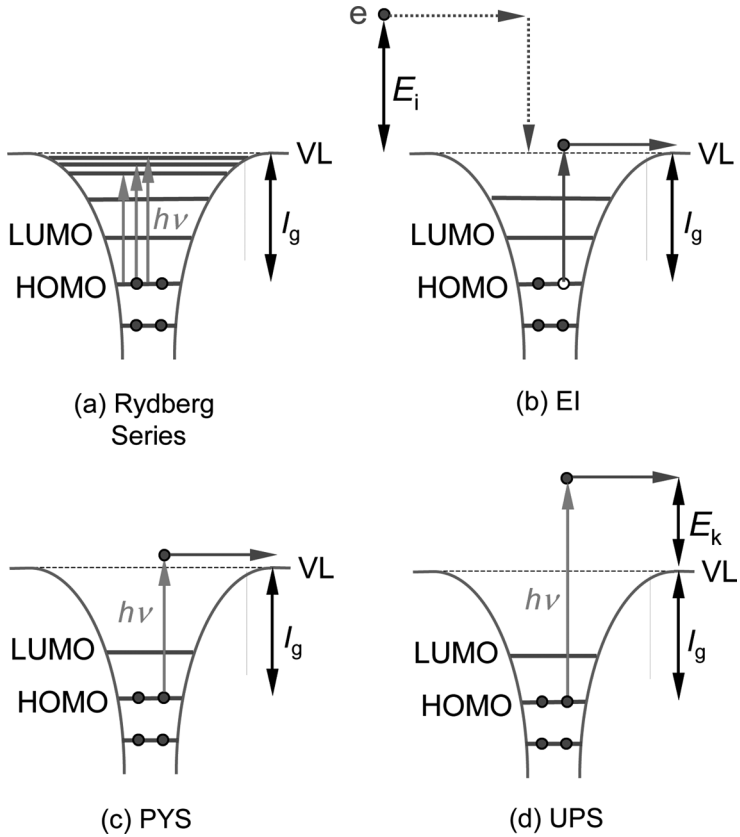

FIGURE 2 Principles of methods for determining the gas phase ionization energy (I_g) of a molecule. (a) Rydberg series, (b) electron impact (EI) mass spectrometry, (c) photoionization yield spectroscopy (PYS), and (d) ultraviolet photoelectron spectroscopy (UPS). VL denotes the vacuum level, and E_i stands for the energy of incident energy of irradiated electron.

the determination of the ionization energies for the ionization from deeper orbitals, such ambiguity is rather high. In the data for benzene [14] in Figure 3(b), the arrows indicate the energies suggested by the authors as the ionization energies of different MOs, but they do not correspond well with those for more reliable UPS data in Figure 3(d).

(c) Photoionization Yield Spectroscopy (PYS) [15]

In this method, cation formation yield at photon impact is followed as a function of photon energy $h\nu$, and I_g is identifies as the minimum

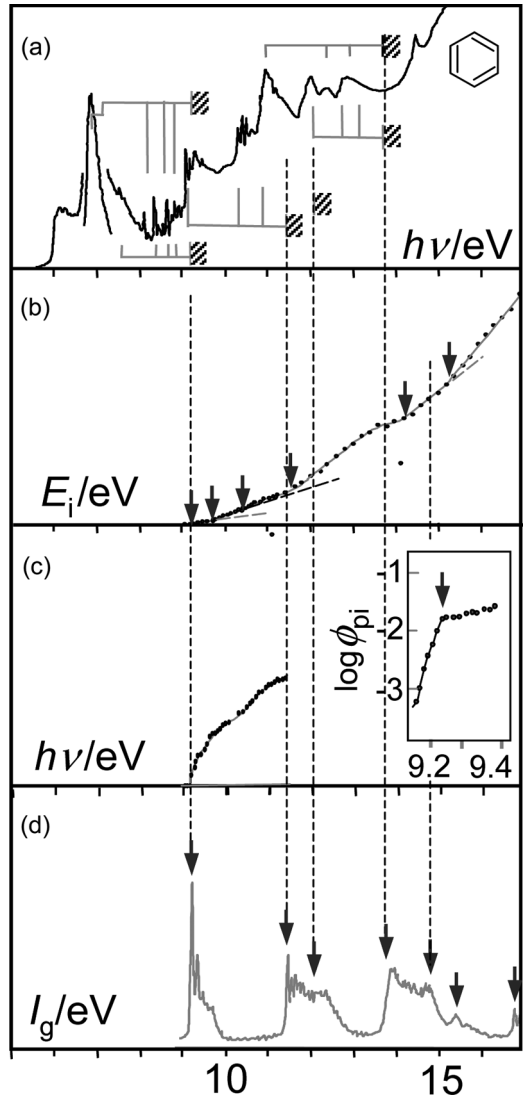

FIGURE 3 Comparison of the experimental data for determining the gas phase ionization energy (I_g) of benzene. (a) Rydberg series analysis [12], (b) electron impact (EI) ionization [14], with the suggested ionization energies of deep MOs by the authors are indicated by arrows, (c) photoionization yield spectroscopy (PYS), with the data plotted in the linear scale [19] and logarithmic scale (inset) [15] are shown, and (d) ultraviolet photoelectron spectroscopy (UPS) [21], with the arrows indicating the widely accepted ionization energies of deeper levels.

photon energy for ionization, as shown in Figure 2(c). The obtained value corresponds to adiabatic ionization energy. Unlike EI, the onset is usually clear, as rationalized by theoretical consideration [16,17], and the accuracy is high, since the wavelength of light can be fairly easily calibrated. In Figure 3(c), the data for benzene is plotted in linear [18] and logarithmic [15] scales, and the onset is clearly identified as the break indicated by the arrow in the logarithmic plot. As a result of the development of this reliable method by people like Watanabe [15] and Vilesov [18,19] in the 1950s, compilations of reliable I_g values for many molecules were prepared by this technique in the 60s [15,18,19].

(d) Ultraviolet Photoelectron Spectroscopy (UPS) [12,13]

The kinetic energy of photoelectrons at the irradiation of high energy monochromatic light is analyzed in this method, as shown in Figure 2(d). The accuracy is moderately high, and the information of the deeper levels than HOMO can also be obtained. The method was independently developed in 60s by Vilesov [20] and Turner [21], and the introduction of conventional He discharge lamp by Turner [21] made this technique as the major tool for examining the whole occupied electronic structure of molecules and solids. Both adiabatic and vertical values can be obtained from the onset and the peak energies. As an example, the spectrum of benzene [21] is shown in Figure 3(d). Various variations of PYS and UPS, e.g., the use of synchrotron radiation as the light source [22] or the selective detection of zero-kinetic energy (ZEKE) electrons [23] led to further development of these techniques with more accurate values of I_g and comprehensive knowledge about the occupied electronic structure of molecules.

(e) Indirect Methods

As more indirect methods, electrochemical oxidation potential E_{ox} corresponds to the cation formation, and its value is closely related to the ionization energy [1], though there are various affecting factors such as the solvent effect [24]. Also the energy of charge-transfer absorption in solution is roughly determined by the combination of the ionization energy of the electron donor and the electron affinity of the electron acceptor, and the comparison of absorption among various complexes enables an estimation of these energy parameters [25]. These methods have been widely used for a rough estimation of the values of I_g, in particular by the people without access to sophisticated PYS or UPS instruments. More detailed description about them, together with a compilation of the values of I_g and E_{ox} for fundamental and electronically functional materials can be found in Reference [1].

2. Gas Phase Electron Affinity (A_g)

The determination of the electron affinity of molecules has been much more difficult than that for the ionization energy. This is mainly because an excess electron must be added to the system, in contrast to the case of ionization energy where an electron existing in the molecule can be used as a probe to be emitted. Thus the more or less reliable direct information has become available only in the 60s and 70s, by techniques like magnetron method (thermal electron from a filament + molecule + magnetic filed; applicable for $A_g > 0.8$ eV) [26], electron capture detector (ECT) method (thermal electron + molecumolecule + pulsed voltage; for $0.1 < A_g < 0.9$ eV) [27], and alkali metal beam (AMB) method (electron transfer from alkali metal to the molecule) [28]. Then thermal charge transfer (TCT) method described below was developed in 1970s and 80s, being extensively used for determining the relative values of A_g for important electron acceptors [29]. The methods and results are discussed in a review reporting the status by 1980s [2], where the data of 130 molecules are listed. The values obtained in these equilibrium type experiments correspond to adiabatic values. In parallel, electron transmission spectroscopy (ETS) was developed in 1970s for probing the vacant levels *above* the vacuum level of various molecules [7]. Unfortunately ETS cannot be used for obtaining A_g of electronically functional molecules with LUMO *below* the vacuum level. Thus the situation is still less satisfactory than the case of ionization energy. However, the recent development of the photodetachment spectroscopy (PDS) of anions [30] is changing the situation, and we now have rather good chance of obtaining reliable set of data at least for medium sized molecules in near future [9,30]. The principles of these spectroscopic methods are schematically depicted in Figure 4. Below we will discuss these recent methods.

(a) Thermal Charge Transfer

Kebarle and Chaudhurry [29] have developed a high-pressure mass spectrometric technique in 1980s, where the electron transfer equilibrium constant between a molecule and an anion can be determined as a function of temperature. From the slope relative to the inverse of temperature, they could determine the relative values of A_g with respect to that for SO_2 for about 120 molecules. Similar technique was developed using electron cyclotron resonance (ECR) [31]. As mentioned above, this method gives adiabatic values of A_g.

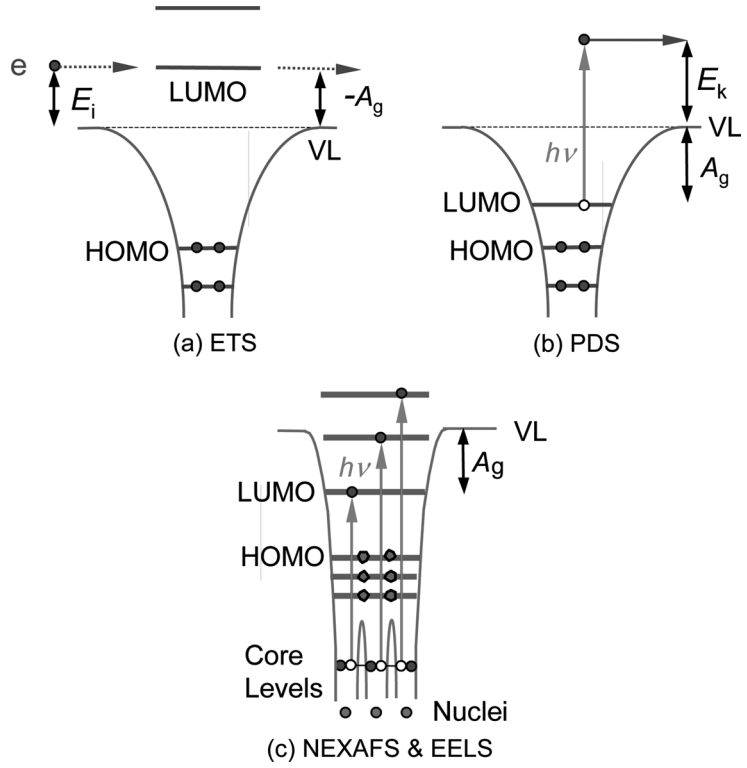

FIGURE 4 Principles of the spectroscopic methods for determining the gas phase electron affinity (A_g) of an isolated molecule. (a) electron transmission spectroscopy (ETS), (b) photodetachment spectroscopy (PDS), and core excitation spectroscopies (near-edge X-ray absorption fine structure (NEXAFS) spectroscopy and electron energy loss spectroscopy (EELS)). VL denotes the vacuum level, E_i denotes the incident energy of injected electron, and E_k is the kinetic energy of photoelectron.

(b) Electron Transmission Spectroscopy (ETS) [7,32]

This method has been used for determining the LUMO and higher vacant MOs *above* the vacuum level. The transmission of electrons injected into a gas is measured as a function of electron energy, as depicted in Figure 4(a). When the energy of injected electron E_i matches the energy of the vacant MO, the electron can be temporally captured in the MO, and loses the memory of the injected direction, leading to the decrease of transmission. Starting from the famous Franck-Hertz experiment [33], this method has been successfully used for determining A_g for small molecules such as N_2 and benzene, with

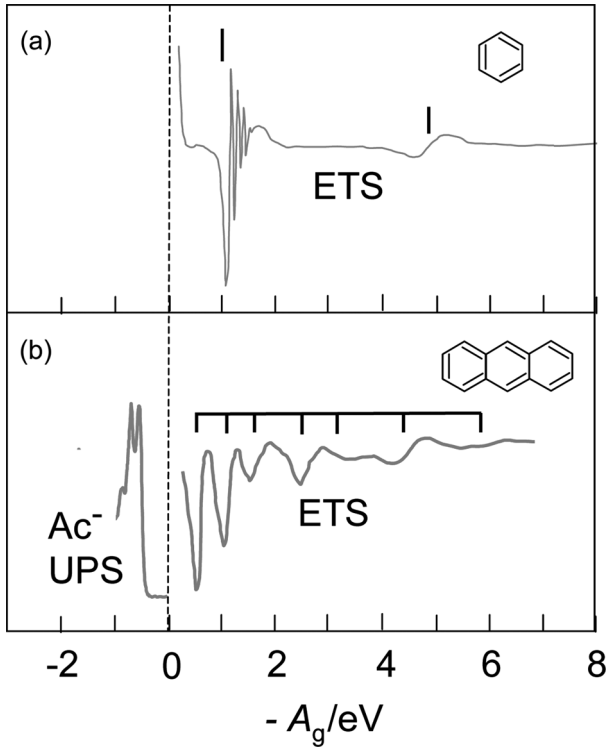

FIGURE 5 Spectroscopic data for the determination of gas phase electron affinity (A_g). (a) electron transmission spectroscopy (ETS) of benzene [7], and (b) photodetachment spectroscopy (PDS) of anthracene anion (Ac^-) [37] and ETS for anthracene vapor [34]. The energies of the vacant levels in the ETS spectra in the derivative form are shown by the vertical bars. Note that the energy axis is the negative of A_g. Benzene and anthracene have negative and positive values of A_g for the LUMO, respectively.

applications to various organic molecules since 1970s [7,32]. In Figure 5(a) and 5(b), the ETS spectra of benzene [7] and anthracene [34] are shown, respectively. For enhancing the spectral features, the spectra are shown as the derivative of the transmission with respect to E_i. In principle, both adiabatic and vertical values are obtained by analyzing the spectral shape of the observed features. The LUMO and the vacant uppermost π orbital of benzene can be clearly seen at $A_g = -1.1$ eV and -4.8 eV, and number of levels of anthracene can be seen. Unfortunately, however, the LUMOs of large molecules with electronic functions are mostly *below* the vacuum level, limiting the usefulness of this method.

(c) Photodetachment Spectroscopy (PDS)

In this method, UPS is applied to a molecular anion M^- to cause a process of

$$M^- + h\nu \Rightarrow M + e^- \tag{3}$$

(see Fig. 4(b)), which is a reverse process to the electron attachment

$$M + e^- \Rightarrow M^- + A_g. \tag{4}$$

Thus the value of I_g for the anion is the value of A_g for the neutral molecule. Such experiment can be precisely carried out using lasers, since the required photon energy is usually small. Although the application of this method for electronically functional molecules has been somewhat limited in the early days [35], there are recent reports from1990s on the anions for large electronically important molecules such as acenes [36,37], *p*-benzoquinone [38], C_{60} [39], and nucleic acid bases [40], and reliable data may become accumulated also for other molecules in near future. In principle, this method gives both adiabatic and vertical values, though the vertical value corresponds to the equilibrium molecular geometry of the anion. An example of santhracene is shown in Figure 5(b), indicating the value of $A_g = 0.53$ eV [36].

(d) Near-edge X-ray Absorption Fine Structure (NEXAFS) Spectroscopy and Electron Energy-Loss Spectroscopy (EELS)

As another possibility for probing the unoccupied states, we can examine core excitation spectroscopies dealing with the transitions from core levels to various vacant levels, as shown in Figure 4(c). Such high-energy spectroscopies can be performed either by using soft X-ray photons or high-energy electrons. The former is usually performed using synchrotron radiation, and called *near-edge X-ray absorption fine structure* (NEXAFS) spectroscopy [41]. The latter is *electron energy loss spectroscopy* (EELS) [42]. The spectra are rather similar for vapor and solid states, reflecting the localized nature of core excitations.

One may imagine that the observed spectrum can be regarded as a simple replica of the density of unoccupied states (DOUS) due to the almost similar energies of the core levels, and there are number of reports based on this naive assumption, in particular for the solid state. Unfortunately, this assumption is not true for most of the cases. Since there are more trials for directly deducing the DOUS for solids rather than isolated molecules, we will discuss them later in relation to the determination of solid state electron affinity.

(e) Indirect Methods

Besides the methods discussed above, we can also mention the use of reduction potentials [24] and the charge-transfer spectra [25] as indirect methods, in correspondence to the case of I_g.

ENERGY PARAMETERS OF ORGANIC SOLID

As seen in Figure 1(b), the energetics of carrier formation in an organic solid can be discussed in terms of two leading parameters, i.e., ionization energy (I_s) and electron affinity (A_s), where s stands for the solid. As in the case of molecules, they correspond to the effective orbital energies of the HOMO and LUMO, respectively. We note, however, that their values differ from those for the gas phase (I_g and A_g) due to the electronic polarization of electronic clouds in the medium surrounding the ionized molecule [43,44]. This energy stabilization is called *polarization energy*. Thus the values for the gas and solid states are related with the relation

$$I_s = I_g - P_+, \tag{5}$$

$$A_s = A_g + P_-, \tag{6}$$

where P_+ and P_- are the polarization energies for a molecular cation and anion, respectively. For solids with appreciable band width by strong intermolecular interaction, the broadening of the HOMO and the LUMO also contribute to the lowering of I_s and the increase of A_s. Due to these complexities, the distinction between the *adiabatic* and *vertical* values becomes mostly meaningless, although the interpretation of the spectral shape is still an important subject in obtaining meaningful energy parameters from experiments.

Other energy parameters are also used for discussing the energetics in organic solids and interfaces. The Fermi level plays an important role in discussing the electrical equilibrium and possible band bending at the interface. Another is the energy of VL. We note that the energy of VL just outside the surface as shown in Figure 1(b), which can be experimentally determined, is different from the energy of VL infinitely far from the system, which can be used as the energy origin [45]. This is due to the electrostatic dipole layer formed at the surface, and can vary depending on the surface structure. This leads to the well-known face dependence of work function Φ, which is another important energy parameter. For example, the values of Φ for the (100), (110), and (111) surfaces of W are 4.63, 5.25, and 4.47 eV, respectively [46]. More detailed discussion of the physical meaning of VL is described in Reference [45]. For discussing the energetics at

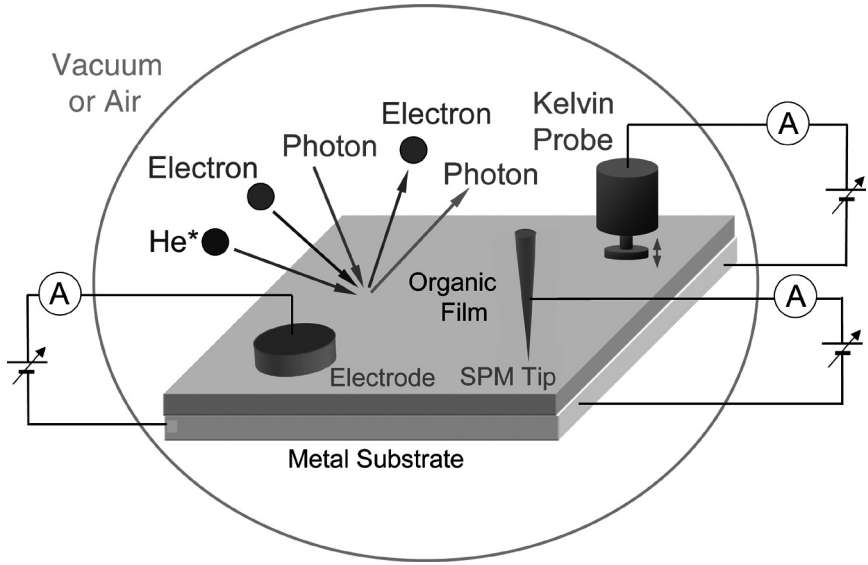

FIGURE 6 Schematic illustration of the various methods for determining the energy parameters of an organic solid. He* denotes electronically excited metastable He atom.

organic/metal interfaces, the location of the VL relative to the electronic structure of the metal becomes important. Thus the determination of the VL energy and Φ is also necessary.

For determining these energy parameters, number of techniques are used, as schematically illustrated in Figure 6. Usually a thin organic film is prepared on a metal surface, under (ultrahigh)vacuum or under various gas atmosphere, and the system is studies by various techniques, which can be roughly categorized into two. One is spectroscopic methods, in which stimulation like photons or electrons is impinged upon the sample, and the response such as photons and electrons are detected. The other is electrical measurements, where electrical current is measured in various types of setups. In the following, we will discuss these methods.

1. Solid State Ionization Energy (I_s)

As in the case of gas phase, the determination of solid state ionization energy is easier than that of the electron affinity. Methods similar to those for the vapor phase, i.e., PYS and UPS, have been used from the early days. As a variation, recently 2-photon photoemission

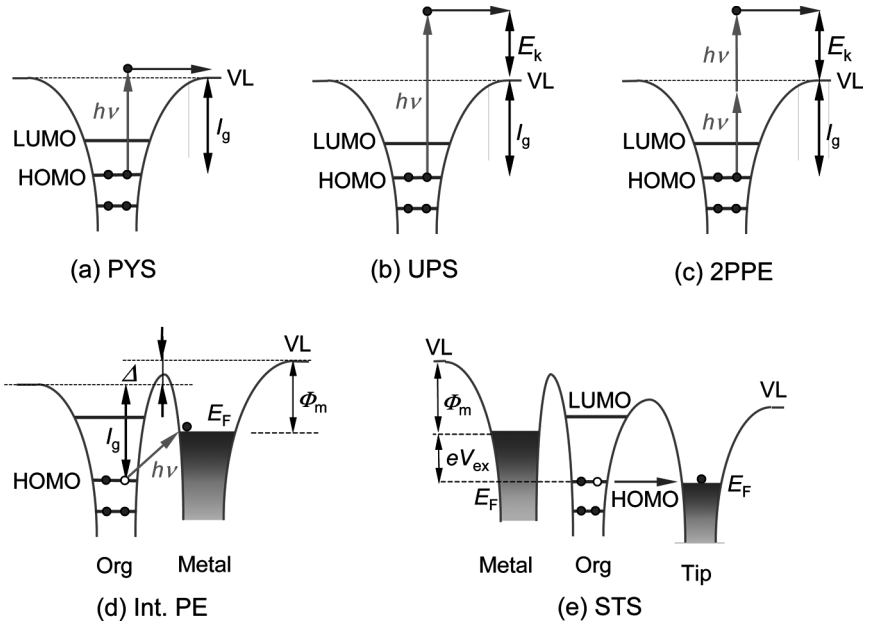

FIGURE 7 Principles of the experimental methods for determining the solid state ionization energy (I_s). (a) photoemission yield spectroscopy (PYS), (b) ultraviolet photoelectron spectroscopy (UPS), (c) two photon photoemission spectroscopy (2PPE), (d) internal photoemission, and (e) scanning tunneling spectrocopy (STS). VL: vacuum level, E_k: kinetic energy of photoelectron, Φ_m: work function of metal substrate, E_F: Fermi level of the metal substrate, Δ: vacuum level shift at the interface due to dipolar layer formation, e: elementary charge, V_{ex}: external voltage.

(2PPE) technique is also emerging as a powerful new method. Aside from these spectroscopic methods, electric measurements of internal photoemission from metal electrode into organic layer was used from the early days of 1960s for deducing the HOMO energy relative to the Fermi level of the metal. The principles of these methods are schematically illustrated in Figure 7.

(a) Photoemission Yield Spectroscopy (PYS) and Millikan Apparatus

As in the case of free molecules, the technique of PYS [47] has been used from the 1960s as a conventional method of directly determining I_s, as shown in Figure 7(a). The developments until 1980s are described in Reference [1]. As an example, the data for naphthacene is shown

in Figure 8(a). The way of extrapolating the yield to zero is discussed based on a model of photoelectric emission [48], and the use of cube-root $Y^{1/3}$was proposed to be the best. This also gives reasonably good agreement with the results of UPS. The bottom panel of Figure 8(a) shows

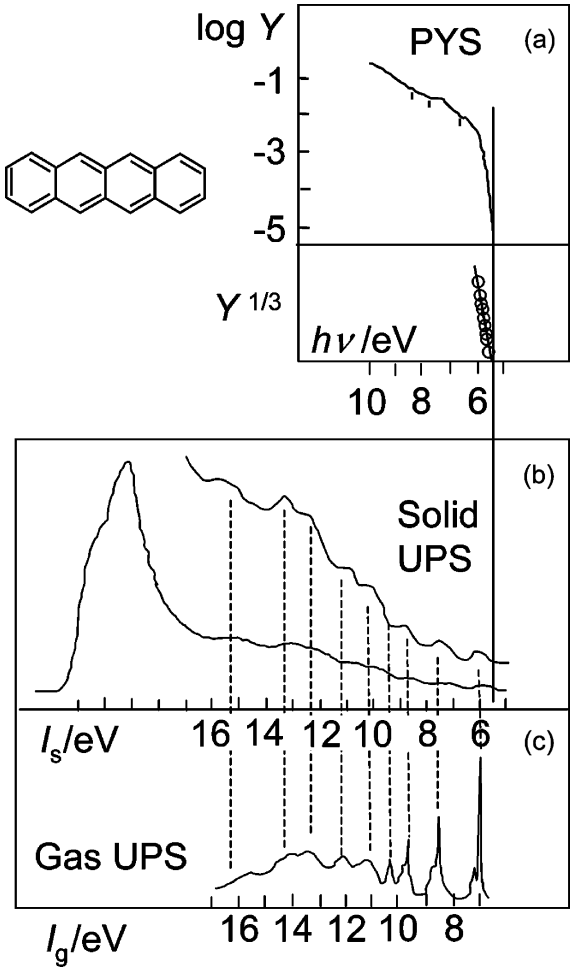

FIGURE 8 Spectroscopic data for the determination of solid state ionization energy (I_s) for naphthacene. (a) photoemission yield spectroscopy (PYS) [48]. Y stands for the photoelectron yield. (b) and (c): ultraviolet photoelectron spectroscopy (UPS) by using He I radiation ($h\nu = 21.2$ eV) for thin film (b) [59] and vapor (c) [60], respectively. Note the 1:1 correspondence between the spectra for the two phases.

the data of naphthacene in this way. As a more special technique for determining I_s, apparatuses similar to that for Millikan droplet experiments have also been used, including the trials for two photon photoemission experiments [49,50]. The early data in 1960s including the values of P_+ are compiled, e.g., in Refs. [51]. The later compilations are described below in the section of UPS.

In 1980s, a conventional PYS instrument for determining I_s in air has become commercially available [52], by which I_s can be measured in air. In this instrument, the photoelectrons are captured by oxygen molecules in air, and the resultant oxygen anions are accelerated by an electric field to cause an avalanche pulse, which is detected by a special detector [53]. In air, the range of measurement is limited to below 6.2 eV due to the light absorption by air, while it is extended beyond this limit in more recent version by replacing the atmosphere by more transparent N_2 gas [52,54]. This type of instruments got popularity in the community of organic devices, and recently a compilation of the values of I_s for about 316 organic materials measured by the above-mentioned commercial instrument is available [55].

Recently, the capability of the PYS measurements have been further put forward by us and Ishii and coworkers by direct measurement of hole current instead of the pulse counter [56,57]. Thus there is no need for oxygen atmosphere, and the instrument can be used both under gases and in vacuum *for the same specimen*. Thus this can be applied for the precise examination of the effect of atmosphere on I_s. The first example for titanyl phthalocyanine is reported by Honda *et al*. in this volume [56].

(b) Ultraviolet Photoelectron Spectroscopy (UPS) and Metastable Atom Electron Spectroscopy (MAES)

The principle of UPS for a solid, shown in Figure 7(b), is similar to that for the gas phase in Figure. 2(b). Its application for determining I_s using low energy photons dates back to 1960s [58]. By the employment of the high-energy He light source (21.2 eV) in late 70s, UPS became the standard method of I_s determination, partly because they became commercially available. By using the high photon energy, it became also possible to probe the major part of the valence states. These studies showed that the spectra for the vapor and solid usually show good one-to-one correspondence, as seen in Figure 8(b) [59] and (c) [60] for naphthacene, reflecting the preservation of the electronic structure of a molecule in the solid state. At the same time, we note that the good correspondence is obtained with a shift of the energy axes by about

1 eV, revealing the effect of the polarization energy P_+ described above. The compound dependence of P_+ was extensively studied by Sato [61], and the compilation of the data of I_g, I_s, and P_+ by 1980s including 120 compounds are given in Reference [1]. Another critical collection of data including A_g and A_s is also found in Reference [62].

In Figures 8(b) and (c), we also note the fairly large peak width in the spectrum for the solid. Several possible origins are proposed: the variation of the polarization energy between the bulk and the surface, coupling with intra- and intermolecular vibrations, and the broadening due to the uncertainty principle due to the finite hole lifetime, and so on [63,64]. Their clarification is still a subject of hot debate, and people are usually using the onset, rather than the peak energy, as the value of I_s for discussing the electronic processes. We note that the groups of Ueno [65] and Umbach [66] recently performed detailed high-resolution UPS studies for well-defined systems by carefully depositing organic molecules on graphite and metal surfaces, respectively, and the data of this kind will be useful for getting further insight into these problems.

In early 80s, UPS has become used to obtain more detailed information about the electronic structure, such as the *intra-* and *inter-*molecular energy band dispersion relation $E = E(k)$ through the combination of well-oriented samples and angle-resolved UV photoelectron spectroscopy (ARUPS), where the kinetic energy distribution of photoelectrons emitted into specific steric angle is analyzed [67].

As a special variation of UPS, the incident photon can be replaced by electronically excited metastable atom of rare gas (usually He) (see Fig. 6). Since the metastable atom cannot penetrate into the organic layer, this metastabel atom electron spectroscopy (MAES) or Penning ionization electron spectroscopy (PIES) has extreme surface sensitivity, and can be used for examining molecular orientation or the surface coverage of substrates [68]. As a method of determining the ionization energy, MAES has a little ambiguity due to the variation of the transferred energy to the molecule at various distance between the He metastable atom and the solid.

(c) Two-Photon Photoemission Spectroscopy (2PPE)

In the last decade, two-photon photoemission spectroscopy using strong laser light has been developed as another powerful variation of UPS by several workers such as Zhu [69], Matsumoto [70], and Munakata [71], following the related work by the group of Harris [72] for smaller molecules regarded as simple dielectric medium. Its principle is illustrated in Figures 7(c) and 9(d).

Even when a single laser (photon energy $h\nu$) is used, we can consider various two-photon processes leading to photoemission [69]. As processes entirely in the organic solid, we can consider the absorption of the second photon with and without relaxation after the absorption of the first photon (Fig. 7(c)). For excitation without relaxation, we can simply analyze the spectrum as an analogue of a single-photon UPS spectrum using $2h\nu$ as the excitation energy. When $h\nu$ is changed by $\Delta(h\nu)$, the kinetic energy of photoelectron from a specific occupied state will be changed by $2\Delta(h\nu)$. For molecules at the interface with a solid substrate, we can also think about the electron injection from the substrate by the first photon leading to anion formation, which is followed by the photoemission of the injected electron by the second photon. Such a process will be discussed later as a method of determining the electron affinity of the solid. Also we mention that the combination of two lasers with different energies (two-color experiments) is also possible, giving further degree of freedom of the experiments.

(d) Internal Photoemission

This method was used in early studies of the electronic structure of organic solids in contact with metal electrode [73]. As shown in Figure 7(d), electrons are excited from the HOMO to the vacant state of a metal electrode contacting the organic material. This hole injection is detected as the photocurrent, and I_s is deduced by adding the onset photon energy to the work function of the metal. Similar measurement can be performed for electron injection from the metal into the LUMO of the organic layer for deducing A_s, as described below. This method contains some ambiguity due to the possible dipole layer formation and the difference of work function between the metal and the organic material [45], but it is still useful for estimating the hole injection barrier, and used for such purpose, e.g., for some conducting polymers [74].

2. Solid State Electron Affinity (A_s)

The determination of A_s has been rather difficult, as in the case of A_g, and internal photoemission in the electron injection mode was at first the almost only way of directly deducing A_s. This situation was changed by the introduction of inverse photoemission (IPES) in the 80s and 2PPE in 90s. Also the recent development of photodetachment spectroscopy of negatively charged molecular clusters offers a new way of estimating A_s. Besides these techniques, there are recent reports using NEXAFS (near-edge X-ray absorption fine structure) spectroscopy as a

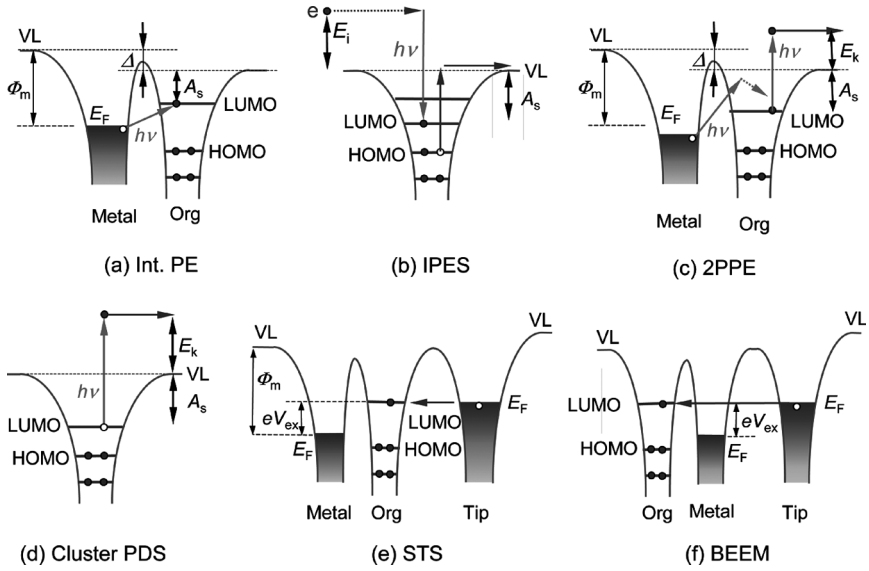

FIGURE 9 Principles of the experimental methods for determining the solid state electron affinity (A_s). (a) Internal photoemission, (b) inverse photoemission spectroscopy (IPES), (c) two photon photoemission spectroscopy (2PPE), (d) photodetachment spectroscopy (PDS) of cluster anion, (e) scanning tunneling spectroscopy (STS), and (f) ballistic electron emission microscopy (BEEM). VL: vacuum level, E_k: kinetic energy of photoelectron, Φ_m: work function of metal substrate, E_F: Fermi level of the metal substrate, Δ: vacuum level shift at the interface due to dipolar layer formation, e: elementary charge, V_{ex}: external voltage.

tool for probing the unoccupied states of organic systems, but the use of this method needs significant care, as described below. The principles of these methods are schematically Illustrated in Figure 9.

(a) Internal Photoemission

Internal photoemission, just described above, can also be used for determining the LUMO energy relative to the Fermi level of the contacting metal electrode (see Fig. 8(a)). The electron injection barrier can be deduced as the onset photon energy of the photocurrent. For performing such experiments, low work function metal (e.g., alkali metal) is necessary, and possible complexation between the metal and the organic material make the analysis somewhat difficult. These experiments (e.g., Ref. [75]) formed the early trials for deducing the LUMO energy.

(b) Electron Transmission Spectroscopy (ETS)

As in the gas phase (see Fig. 4(a)), ETS can be used for examining the electronic structure of organic solids *above* the vacuum level. Such studies were extensively carried out, in particular by the group of Sanche [76]. If the solid has the LUMO above the vacuum level, as in the case of long-chain alkanes [77], the value of A_s can be directly determined. The estimation of A_s for π-conjugated system with LUMO *below* VL was also tried, but in an indirect way [78].

(c) Inverse Photoemission Spectroscopy (IPES)

In this technique, electrons are injected into the solid, and the radiative transition to lower vacant MOs are detected (see (Fig. 9(b)) using a bandpass filter or a monochromator [79]. Its application to organic solids was not so easy due to the heavy radiation damage by the electron beam. Still it has been applied to organic solids from1980s by Koch and collaborators [80,81] and the group of Weaver [82], and after some interval (with the exception of fullerenes [83]), it was revived in the late 90s [84–86], and now used by several groups in the world. In Figure 10(b), the IPES spectrum of anthracene [81], taken by scanning the incident electron energy with monitoring the light intensity at a fixed photon energy of $h\nu = 9.5\,\text{eV}$, is shown. For comparison, the data for anthracene vapor in Figure 5(b) are shown in Figure 10(c), with a shift of 1.0 eV between the energy scales of A_s and A_g. We see a good correspondence between the gas and solid state data, verifying that the unoccupied electronic structure, even above the vacuum level, is fairly well preserved. The energy scale shift corresponds to the polarization energy P_- for an anion, and the magnitude of 1.0 eV is similar to that for P_+ [61]. In Figure 10(f), the spectrum for tris(8-hydroxyquinoline)aluminum (Alq_3) [84] is also shown.

(d) Two-photon Photoemission (2PPE) Spectroscopy

The 2PPE method was already described as a method for determining I_s. As one of the possible processes in the experiment on an organic film on metal substrate, an electron may be injected from the metal into the LUMO of the organic layer to form an excess electron (see Fig. 9(c)). The following excitation by the second photon can emit the electron in the LUMO, and the energy of the LUMO, which corresponds to A_s, can be determined [69]. In such experiments, the change of the kinetic energy of a peak at the photon energy change $\Delta(h\nu)$ will be $\Delta(h\nu)$, in contrast to the case of 2-photon emission in the organic solid, where the shift is $2\Delta(h\nu)$. Such experiments are

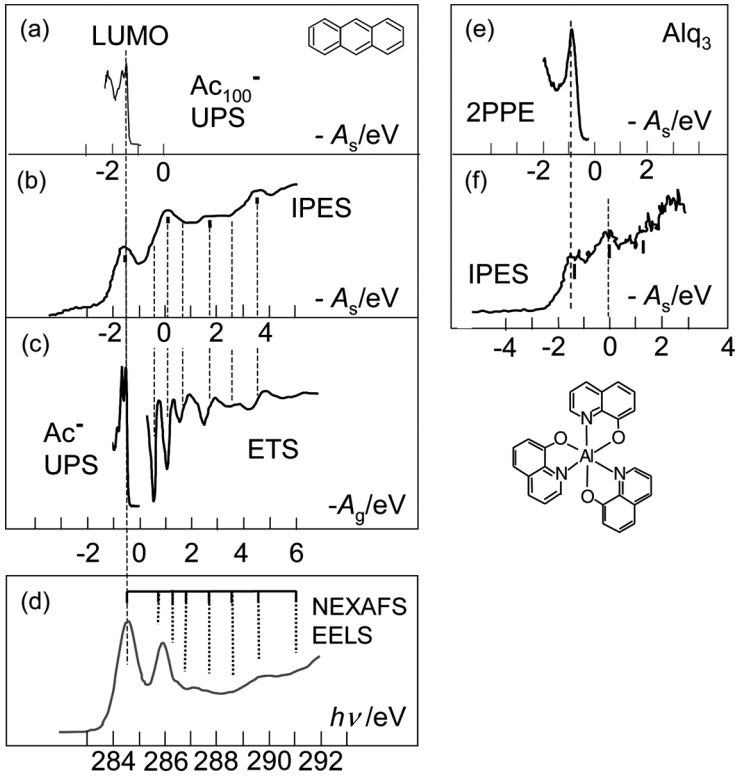

FIGURE 10 Spectroscopic data for the determination of solid state electron affinity (A_s) for anthracene (Ac) and tris(8-hydroxyquinolino)aluminum (Alq_3). (a) Photodetachment spectroscopy (PDS) of anthracene 100-mer anion (Ac_{100}^-) [37], (b) inverse photoemission spectroscopy (IPES) of anthracene solid [81], (c) photodetachment spectroscopy (PDS) of anthracene vapor anion (Ac-) [37] and electron transmission spectroscopy (ETS) of anthracene vapor [34], (d) electron energy-loss spectroscopy (EELS) of anthracene vapor [95], (e) two photon photoemission spectroscopy (2PPE) of Alq_3 solid [88], and (f) IPES of Alq_3 solid [85].

performed in these a few years for solids like C_6F_6 [87] and Alq_3 [70], and this technique may become a useful tool for determining A_s, though such temporary negative state is not always observed, as in the case of perylenetetracarboxylic anhydride (PTCDA) [88]. As an example, the data for Alq_3 [69] is shown in Figure 10(e). The LUMO energy agrees well with that observed in the IPES spectrum [85] in Figure 10(f).

(e) Photodetachment Spectroscopy (PDS) of Molecular Clusters

Recently, UPS experiments for negatively charged large molecular clusters have become possible [37,89]. In such studies, the electron affinity can be determined for molecular clusters (see Fig. 9(d)) with well specified molecular numbers up to ~100. Thus the evolution of the electronic structure from an isolated molecule to that of a molecular solid can be precisely followed as a function of molecular number. The values for sufficiently large molecular number becomes almost constant, and they well correspond to the value by IPES. Thus this method may offer an entirely new reliable method for determining the value of A_s. In Figure 10(a), the spectrum of anthracene 100-mer [37] is shown. The LUMO energy agrees well with that from IPES in Figure 10(b), although the peak width in the IPES spectrum is large, and the analysis of the peak width is necessary.

(f) Near-edge X-ray Absorption Fine Structure (NEXAFS) Spectroscopy and Electron Energy-Loss Spectroscopy (EELS)

As already mentioned above in relation to the gas phase electron affinity, there are trials for using core excitation spectroscopies such as near-edge X-ray absorption fine structure (NEXAFS) spectroscopy [41] and high-energy electron energy-loss spectroscopy (EELS) [42] (see Fig. 4(c)) as a direct probe of the unoccupied electronic structure. They are based on a naïve expectation that the observed spectrum can be regarded as a simple replica of the density of unoccupied states (DOUS) due to the almost similar energies of the core levels.

Unfortunately, however, the energies of the core-excited states are significantly affected by the interaction between the core hole and the excited electron (core excitonic effect), which is much dependent on the excitation site and the pattern of the vacant MO into which the core electron is excited [90,91]. This leads to a significant deviation of the spectrum from the DOUS, practically making this method useless for the quantitative examination of the DOUS. The observed spectrum may reflect the contribution of the element to the DOUS only in the case where all the sites for an element are equivalent, e.g., C in graphite [92] and C_{60} [93], and N in metalloporphyrins [94].

As an example, the gas-phase spectrum of anthracene in the vapor phase [95] is shown in Figure 10(d). We note that the core-excitation spectrum of molecular solid is similar to that of the vapor phase, reflecting the localized nature of the electronic excitation. The energy axis is adjusted to align the lowest energy peak with the LUMO in the spectra in Figures 10(a)–(c). We see that the spectral features show only poor correspondence with those in Figures 10(a)–(c) shown on

the horizontal bar of Figure 10(d). Actually detailed theoretical analysis showed that the lowest energy peak in the EELS spectrum consists of several excitations with different energies from 4 inequivalent sites to the LUMO. More distinct deviation from IPES spectra are also reported for other aromatic hydrocarbons.

3. Energy of the Vacuum Level (VL)

The energy of the vacuum level can be directly determined by the following two major methods. The principle of these methods are illustrated in Figure 11.

(a) UPS

The low kinetic energy cutoff of a UPS spectrum corresponds to the zero kinetic energy defined by the vacuum level of the solid [96], as shown in Figure 11(a). Thus we can directly locate the energy of the vacuum level with respect to the various states probed within a series of UPS measurements, e.g., the Fermi level of the metal substrate. Similar determination can be also made by using an electron injection apparatus such as low-energy electron diffraction (LEED). In Figure 12(a), the shift of the vacuum level Δ at the deposition of Alq_3 on Au [97] is shown. The abscissa is the energy of vacuum level relative to the Fermi level of the metal $\varepsilon_{\mathrm{vac}}^{\mathrm{F}}$ shown in Figure 11(a). The shift to the left corresponds to the lowering of the vacuum level.

(b) Kelvin Probe [98]

In this method, a movable reference electrode is placed in front of the sample surface, and it is connected with the sample substrate via an external circuit with an ac ammeter and an external voltage (V_{ex}), as shown in Figure 11(b). When the energies of the vacuum levels are different by ΔV between the electrode and the surface, a pair of positive and negative charges ($+Q$ and $-Q$) appear at the confronting surfaces, whose amount is defined by the equation of a capacitor:

$$Q = C\Delta V, \tag{7}$$

where C is the capacitance defined by the geometrical arrangement. By vibrating the reference electrode, we can modulate the capacitance, and hence the amount of charge, inducing an alternative current in the external circuit. As seen in Figure 11(c), the value of ΔV is given by

$$e\Delta V = \Phi_{\mathrm{ref}} - \varepsilon_{\mathrm{vac}}^{\mathrm{F}} - eV_{\mathrm{ex}}, \tag{8}$$

where e is elementary charge, Φ_{ref} is the work function of the reference electrode and $\varepsilon_{\mathrm{vac}}^{\mathrm{F}}$ is the energy of the vacuum level of the organic sample relative to the Fermi level of the metal substrate.

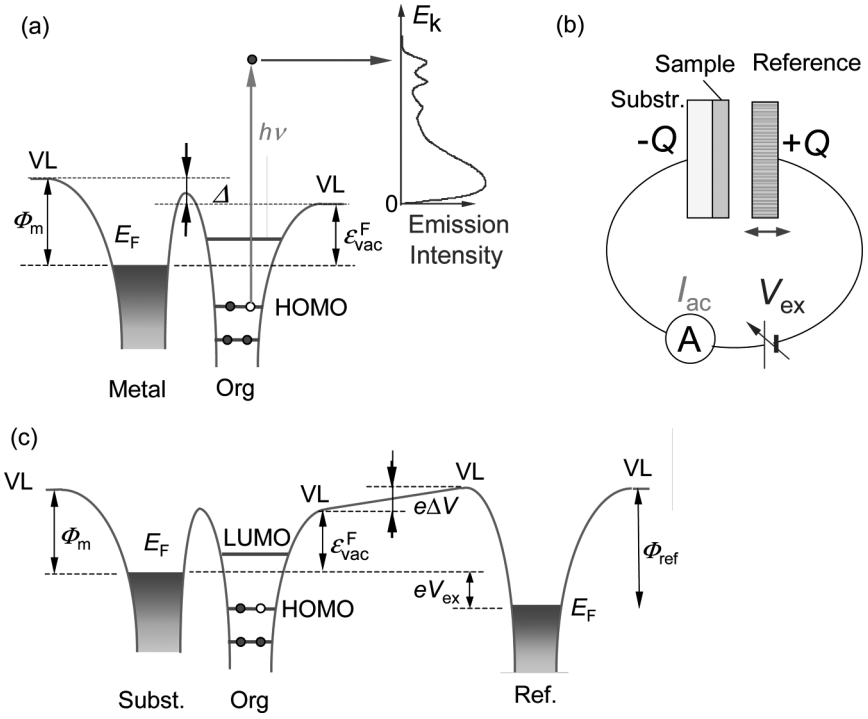

FIGURE 11 Principles of the experimental methods for determining the vacuum level (VL) of solid (ε^F_{vac}) relative to the Fermi level of metal substrate (E_F). (a) ultraviolet photoelectron spectroscopy (UPS). The hatched part of the upper-right curve denotes the contribution of scattered secondary electrons. Φ_m: work function of metal substrate, Δ: shift of the vacuum level by dipole layer formation, (b) setup of Kelvin probe measurement. Q: amount of charge appearing at the surfaces of the sample and the reference electrode, I_{ac}: alternative current in the external circuit, and V_{ex}: external voltage. (c) energy diagram for Kelvin probe measurement. ΔV: surface potential difference between the sample and the reference electrode, e: elementary charge, Φ_{ref}: work function of reference electrode.

The current in the external circuit can be made null by adjusting V_{ex} to make $\Delta V = 0$. From this value of V_{ex}, we can deduce $\Phi_{ref} - \varepsilon^F_{vac}$. With prior measurement of Φ_{ref}, we can also deduce ε^F_{vac}. Examples are shown in Figure 12(b) for clean Ag and Ag modified by self-assembled monolayer (SAM) of $C_8F_{17}(CH_2)_2SH$ [99]. The value of ε^F_{vac} is increased by about 0.8 eV by the surface modification.

This method has been applied to organic semicondutors by Kotani and Akamatu [100,101] in early 70s, and after some interval started

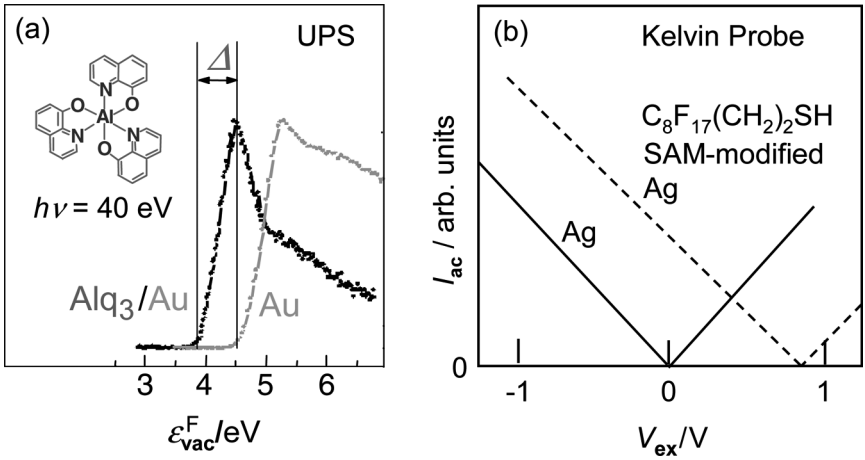

FIGURE 12 Exerimental data for the determination of the energy of the vacuum level (VL) of solid (ε^{F}_{vac}) relative to the Fermi level of metal substrate (E_F). (a) Low-energy cutoff of the UPS spectra clean Au and Au substrate covered with tris(8-hydroxyquinolino)aluminum (Alq_3) [97]. The abscissa is the ionization energy of the solid state, and the shift to the left corresponds to the lowering of the vacuum level. (b) The dependence of the current of Kelvin probe on the external voltage for clean Ag surface and Ag surface covered by self-assembled monolayer of $C_8F_{17}(CH_2)_2SH$ [99].

to be used again [102,103]. In late 90s, Hayashi, Ishii, and Seki performed the first measurements in ultrahigh vacuum for large organic molecules, and applied it for the detailed examination of the Fermi level alignment [104,105] and the group of Kahn also applied this to examine the effect of doping [106].

4. Energy of the Fermi Level (E_F) and Work Function (Φ)

For determining the energy of E_F, there is a major difficulty that this energy can be decided only by relying on the alignment of the Fermi level with that of a contacting solid, e.g., a metal electrode. This is because basically there is no or little level at E_F, and in many cases the energy of E_F can be determined only as the energy of the Fermi level of the contacting metal, which can be observed, e.g., as the Fermi edge in the UPS spectrum. This Fermi level alignment requires the establishment of electrical equilibrium between the two solids, which may not be always established [43,104,105,107,108]. As a useful criterion for examining this, we have proposed that the energy of the Fermi level of metals in contact with the organic layer with respect

to the HOMO or the vacuum level of the organic layer should be independent of the metal [43,104,105,107,108]. In some cases such independence is actually observed with band bending at the interface [104], while the independence is broken for some cases where the well purified organic material is deposited on metals under ultrahigh vacuum (UHV) conditions [105,108].

Once the location of the Fermi level could be determined, the work function Φ can be determined as the energy difference between the vacuum level and the Fermi level. This type of measurements can be carried out by methods like UPS, IPES, and Kelvin probe. We note that the Kelvin probe is primarily a method for determining the energy of the vacuum level, and not the work function. This distinction becomes important when the electrical equilibrium between the organic layer and the metal substrate is not established. Even when the equilibrium is not realized, we can determine the energy of the vacuum level by the Kelvin probe, but cannot determine the work function.

LOCAL PROBES

Finally we will discuss the method for locally determining the energy parameters, which became possible only very recently. For such measurements, we can use the following microscopic methods:

1. Photoelectron Microscopy

There are two types of photoelectron microscopy. In one of them, a microspot of laser light is scanned over the sample surface, and the photoelectrons from each point is analyzed. Basically all the information described above for UPS and 2PPE can be obtained at each point, and the collection of the data shows the spatial variation of various energy parameters.

By combining this method with UPS using a vacuum ultraviolet laser, recently Munakata and collaborators have succeeded in recording the UPS spectra over the surface of Cu phthalocyanine film deposited on polycrystalline Cu film with a lateral resolution of about 300 nm and energy resolution of 30 meV [109]. The observed results show the variation of the HOMO energy by about 0.2 eV and the variation of work function of about 0.4 eV. From the value of work function, the part with high HOMO energy was found to correspond to the Cu(111) surface.

In another type of photoelectron microscopy (PEEM), the photoelectrons emitted from the sample are imaged, with a resolution of a few tens nm and with possible energy analysis [110]. The spatial variation

of I_s often becomes the source of contrast, and some trials for quantitative examination of the energy parameters of functional organic films using this type of microscope is appearing [111].

2. Scanning Tunneling Spectroscopy (STS)

In this method, the technique of scanning tunneling microscopy (STM) is used, with the tip fixed and the voltage between the tip and the sample is scanned (see Figures 7(e) and 9(e)). The tunneling current is increased when the Fermi level of the positively biased tip coincides with an occupied or vacant MO, with the injection of holes or electrons into the sample. Figures 7(e) and 9(e) illustrate the cases where E_F of the tip coincides the HOMO and LUMO energies, respectively. The technique has been successfully applied to various systems such as fullerenes [112] and nanotubes [113]. Also there have been many trials of electric conduction via single molecules using STM and conducting atomic force microscopy (AFM) [114], but the application to thin films functional organic materials has been somewhat limited, Recently, however, reliable data based on careful measurements is coming to be available, and the accumulation of reliable data and their comparison with the more traditional data, e.g., the UPS spectra, will help the establishment of this technique as a probe of the electronic states of molecular solids.

In Figure 13, we show an example of such kind of comparison for PTCDA. In Figure 13(a), the combined UPS and IPES data for thick film [85] are shown. The UPS spectrum for thick 6L film of PTCDA on Ag in Figure 13(b) [66] shows fair agreement with this. On the other hand, the UPS spectrum for thin 1L PTCDA layer [66] differs very much from the one in Figure 13(a), and shows good correspondence with the STS data in Figure 13(c) for PTCDA on Ag(111) surface [115] and in Figure 13(d) for PTCDA on graphite [116]. The UPS and STS data clearly shows the electronic states formed between the HOMO and LUMO levels of PTCDA by the molecule/metal interaction. The STS date even shows the delicate variation of the interfacial electronic states among the molecules in the growing island. Since the STS measurements are not easy to perform for thick layers, we should be careful in recognizing that the system may be strongly affected by the interaction with the substrate, and the obtained data may not simply reflect the electronic structure of molecular solid.

3. Kelvin Force Microscopy (KFM)

The scanning probe microscopic version of the Kelvin probe can be made by using the SPM tip as the vibrating electrode (Kelvin force

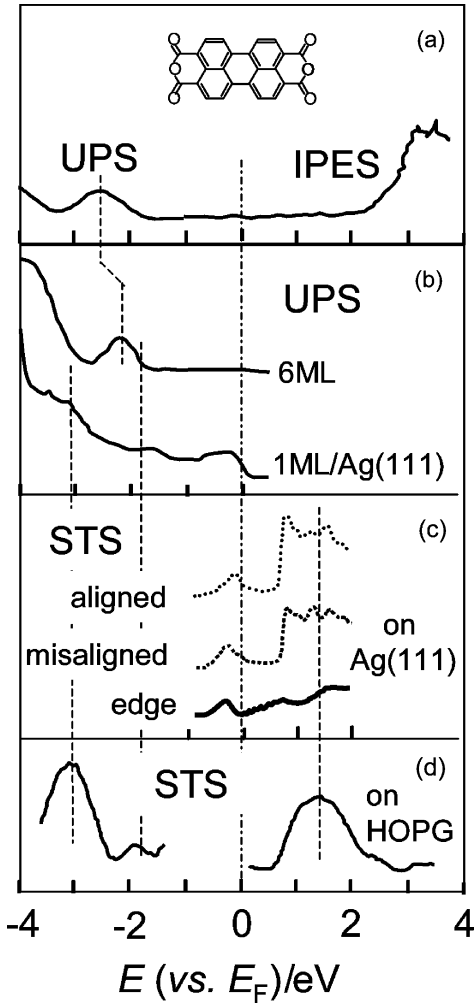

FIGURE 13 Comparison of the structure of occupied and vacant electronic levels of perylenetetracarboxylic acid dianhydride (PTCDA) by scanning tunneling spectroscopy (STS), ultraviolet photoelectron spectroscopy (UPS), and inverse photoemission spectroscopy (IPES). (a) Combined UPS and IPES data for PTCDA film [85]. (b) UPS spectra for one molecular layer (1 ML) and 6 moleclar layers (6 ML) of PTCDA on Ag(111) surface [66]. (c) STS data for PTCDA submonolayer at various types of molecules in the PTCDA island [114]. (d) STS data for PTCDA on graphite [115].

microscopy, KFM) [117]. It has become a powerful tool for examining the local variation of the energy of the vacuum level. Information such as the microsegregation of molecular mixture [118], dependence of the surface potential on the layer thickness [119], and the potential drop at the organic/metal interface [120] have been reported.

4. Ballistic Electron Emission Microscopy (BEEM)

This is a method for probing the LUMO of an organic layer buried under a metallic film [121]. In this sense, this method is a technique examining the interface, as in the case of internal photoemission and STS. The principle is shown in Figure 9(f).

The STM tip is placed in front of the metal layer covering the semiconductor surface, and the tunneling current by the injection of electron/hole into the LUMO of the organic layer through the metal overlayer is measured as functions of the bias between the metal overlayer and the STM tip. From such measurement, we can obtain the injection barrier between the metal Ferm level and the LUMO. This method was at first developed for the inorganic semiconductor/metal interfaces, and a few trials to organic semiconductor interface also recently appeared [122,123].

CONCLUDING REMARKS

In this article, we made an overview on the principle and development of the experimental methods for directly determining the energy parameters of organic molecules and solids. We see that there has been significant development of these methods, in parallel with the development of various applications of organic semiconductors and conductors. Though these developments and their application to various materials, our basic understanding of the electronic structure was much widened and deepened. Also we note that the energy parameters discussed here are also important for discussing the energetics of π- and σ-conjugated polymers, which are also used for organic electronic devices. Although we took examples only from molecular solids, partly because the counterpart data of molecules are available, we can list a few references on polymers [124–126].

We also note that our interest in electronic structure was extended from bulk materials to interfaces. In various organic thin film devices, such as organic light emitting devices (OLEDs), organic solar cells, and organic thin film transistors, organic/metal, organic/organic and other organic interfaces play important roles, and the knowledge about the interfacial electronic structure forms the basis for

understanding and improving the device performances. Most of the techniques described above for the solid state, not only interface-specific methods like internal photoemission, STS, and BEEM, are applicable for the studies of interfaces, and systematic studies of interfaces are rapidly growing. These subjects, which can not be described here due to the limit of space, are discussed e.g., in References [45,105,125–127].

The knowledge obtained in these studies of interfaces are also used in the analysis of the data described in the present article. For example, the presence of the interfacial dipole layer Δ, as shown in Figures 7, 9, 11 was established through these studies [45]. Also we can expect that more detailed and local knowledge will become available through the mutual communication between the field of macroscopic and microscopic measurements. With possible studies of dynamic processes, we can expect that we can get more comprehensive knowledge about the electronic structure of organic electronically functional materials.

REFERENCES

[1] Seki, K. (1989). *Mol. Cryst. Liq. Cryst.*, *171*, 255.
[2] Chen, E. C. M. & Wentworth, W. E. (1989). *Mol. Cryst. Liq. Cryst.*, *171*, 271.
[3] Koopmans, T. A. (1934). *Physica*, *1*, 104.
[4] Karl, N. (2001). In: *Organic Electronic Materials*, Farchioni, R. & Grosso, G. (Eds.), Chapter 6, Springer: Berlin, Heidelberg, 215.
[5] Cauletti, C., Green, J. C., Kelly, M. R., Powell, P., Tilborg, J. V., Robbins, J., & Smart, J. (1980). *J. Electron Spectrosc. Rel. Phenom.*, *19*, 827.
[6] Frost, D. C., McDowell, C. A., Sandhu, J. S., & Vroom, D. A. (1967). *J. Chem. Phys.*, *46*, 2008.
[7] Jordan, K. D. & Burrow, P. D. (1987). *Chem. Rev.*, *87*, 557.
[8] Klots, C., Compton, R. N., & Raaen, V. F. (1974). *J. Chem. Phys.*, *60*, 1177.
[9] http://webbook.nist.gov/chemistry/.
[10] Price, W. C. & Wood, R. W. (1935). *J. Chem. Phys.*, *3*, 439.
[11] Robin, M. B. (1974, 1975, 1985). *Higher Excited States of Polyatomic Molecules*, Academic Press: New York, Vols. 1–3.
[12] Koch, E. E. & Otto, A. (1972). *Chem. Phys. Lett.*, *12*, 476.
[13] Field, F. H. & Franklin, J. L. (1957). *Electron Impact Phenomena and Properties of Gaseous Ions*, Academic Press: New York.
[14] Fox, R. E. & Hickam, W. M. (1954). *J. Chem. Phys.*, *22*, 2059.
[15] Watanabe, K., Nakayama, T., & Mottle, J. (1962). *J. Quant. Spectosc. Energy Transf.*, *2*, 369.
[16] Morrison, J. D. (1957). *J. Appl. Phys.*, *28*, 1409.
[17] Clarke, E. M. (1954). *Can. J. Phys.*, *32*, 764.
[18] Terenin, A. & Vilesov, F. I. (1964). *Adv. Photochem.*, *2*, 285.
[19] Vilesov, F. I. (1963). *Usp. Fiz. Nauk.*, *81*, 669 [in Russian; Eng. Translation: *Sov. Phys. USPEKHI*, *6*, 888 (1964)].

[20] Vilesov, F. I., Kurbatov, B. L., & Terenin, A. N. (1961). *Dokl. Akad. Nauk SSSR*, *138*, 1329.
[21] Turner, D. W., Baker, C., Baker, A. D., & Brundle, C. R. (1970). *Molecular Photoelectron Spectroscopy*, Wiley: London, and references therein.
[22] Hatano, Y. (2002). In: *Chemical Applications of Synchrotron Radiation*, Part I, Sham, T. K. (Ed.), Chapter 2, World Scientific: Singapore, 55.
[23] Mueller-Dethlefs, K. & Schlag, E. W. (1991). *Ann. Rev. Phys. Chem.*, *42*, 109.
[24] Pysh, E. S. & Yang, N. C. (1963). *J. Am. Chem. Soc.*, *85*, 2114.
[25] Mulliken, R. S. & Person, W. B. (1962). *Ann. Rev. Phys. Chem.*, *13*, 107.
[26] Page, F. M. & Moore, G. C. (1969). *Negative Ions and the Magnetron*, Wiley: New York.
[27] Chen, E. C. M. & Chen, E. S. D. (2004). *The Electron Capture Detector and the Study of Reactions with Thermal Electrons*, Wiley & Sons: Hoboken.
[28] Cooper, C. D., Frey, W. F., & Compton, R. N. (1978). *J. Chem. Phys.*, *69*, 2367.
[29] Kebarle, P. & Chaudhury, S. (1987). *Chem. Rev.*, *87*, 513.
[30] Rienstra-Kiracofe, J. C., Tshumper, G. S., Schaefer III, H. F., Nandi, S., & Ellison, G. B. (2002). *Chem. Rev.*, *102*, 231.
[31] Raines, L. J., Moore, H. W., & McIver, R. T. (1977). *J. Chem. Phys.*, *68*, 3309.
[32] Allan, M. (1989). *J. Electron Spectrosc. Rel. Phenom.*, *48*, 219.
[33] Franck, J. & Hertz, G. (1917). *Verh. Dtsch. Phys., Ges.*, *16*, 457.
[34] Burow, P. D., Michejda, J. A., & Jordan, K. D. (1987). *J. Chem. Phys.*, *86*, 9.
[35] Lyons, L. E. & Palmer, L. D. (1973). An early example for tetracyanoethylene. *Chem. Phys. Lett.*, *21*, 442.
[36] Schiedt, J. & Weinkauf, R. (1997). *Chem. Phys. Lett.*, *266*, 201.
[37] Mitsui, M., Kokubo, S., Ando, N., Matsumoto, Y., Nakajima, A., & Kaya, K. (2004). *J. Chem. Phys.*, *121*, 7553.
[38] Schiedt, J. & Weinkauf, R. (1999). *J. Chem. Phys.*, *110*, 304.
[39] Wang, X. B., Ding, C. F., & Wang, L. S. (1990). *J. Chem. Phys.*, *110*, 8217.
[40] Schiedt, J., Weinkauf, R., Neumark, D. M., & Schlag, E. W. (1998). *Chem. Phys.*, *239*, 511.
[41] Stöhr, J. (1992). *NEXAFS Spectroscopy*, Springer: Berlin.
[42] Hitchcock, A. P. (2000). *J. Electron Spectroscopy Rel. Phenom.*, *112*, 9.
[43] Lyons, L. E. (1957). *J. Chem. Soc.*, 5001.
[44] Silinsh, E. A. & Capek, V. (1994). *Organic Molecular Crystals. Interaction, Localization, and Transport Phenomena*, American Institute of Physics Press: New York.
[45] Ishii, H., Sugiyama, K., Ito, E., & Seki, K. (1999). *Adv. Mat.*, *11*, 605.
[46] Stayer, R. A., Mackie, W., & Swanson, L. W. (1973). *Surf. Sci.*, *34*, 225.
[47] Lyons, L. E. & Morris, G. C. (1960). *J. Chem. Soc.*, 5192.
[48] Kochi, M., Harada, Y., Hirooka, T., & Inokuchi, H. (1970). *Bull. Chem. Soc. Jpn.*, *43*, 2690.
[49] Pope, M. (1962). *J. Chem. Phys.*, *36*, 2810.
[50] Gerischer, H. & Ranke, W. (1969). *Z. Naturforsch.*, *24*, 463.
[51] Gutmann, F. & Lyons, L. E. (1967). *Organic Semicondors*, Wiley: New York.
[52] Riken Keiki Co., Ltd., Tokyo (http://www.ac-2.com/).
[53] Kurihata, H. & Uda, M. (1981). *Rev. Sci. Instrum.*, *52*, 68.
[54] Ishii, H. private communication.
[55] Adachi, C., Oyamada, T., & Nakajima, Y. (2006). *Data Book on Work Function of Organic Thin Films* (in Japanese), 2nd Ed., CMC: Tokyo. The term "work function" should read "ionization energy."

[56] Honda, M., Kanai, K., Ouchi, Y., & Seki, K. (2006). *Mol. Cryst. Liq. Cryst.*, *455*, 219–225.
[57] Ogawa, S., Kimura, Y., Ishii, H., & Niwano, M. Proc. 7th European Conference on Molecular Electronics (ECME) 2003.9.10-9.14 Avignon, France.
[58] Vilesov, F. I. & Terenin, A. N. (1960). *Doklady Akad. Nauk SSSR*, *133*, 1060. [Engl. Trans.: (1960). *Sov. Phys. Doklady*, *5*, 840].
[59] Seki, K., Inokuchi, H., & Harada, Y. (1973). *Chem. Phys. Lett.*, *20*, 197.
[60] Clark, P. A., Brogli, F., & Heilbronner, E. (1972). *Helv. Chim. Acta*, *55*, 1415.
[61] Sato, N., Seki, K., & Inokuchi, H. (1981). *J. Chem. Soc. Faraday Trans. 2*, *77*, 47.
[62] Karl, N. (1985). In: *Landort-Börnstein Numerical Data and Functional Relationships in Science and Technology*, Madelung, O., Schulz, M., & Weiss, H. (Eds.), Springer: Berlin and Heidelberg, Vol. 17i, 106.
[63] Salaneck, W. R. (1978). *Phys. Rev. Lett.*, *40*, 60.
[64] Duke, C. B., Salaneck, W. R., Fabishi, T. J., Ritsko, J. J., Thomas, H. R., & Paton, A. (1978). *Phys. Rev.*, *B18*, 5717.
[65] Kera, S., Yamane, H., Sakuragi, I., Okudaira, K. K., & Ueno, N. (2002). *Chem. Phys. Lett.*, *364*, 93.
[66] Umbach, E., Glöckler, K., & Sokolowski, M. *Surf. Sci.*, in press.
[67] Seki, K., Ishii, H., & Ouchi, Y. (2002). In: *Chemical Applications of Synchrotron Radiation*, Sham, T. K. (Ed.), Chapter 8, World Scientific: Singapore, 386.
[68] Harada, Y., Masuda, S., & Ozaki, H. (1997). *Chem. Rev.*, *97*, 1897.
[69] Zhu, X.-Y. (2002). *Ann. Rev. Phys. Chem.*, *53*, 221 and references therein.
[70] Ino, D., Watanabe, K., Takagi, N., & Matsumoto, Y. (2005). *Phys. Rev., B*, *71*, 115427 and references therein.
[71] Munakata, T. & Shudo, K. (1999). *Surf. Sci.*, 433–345, 184 and references therein.
[72] Szymanski, P., Garrett-Roe, S., & Harris, C. B. (2005). *Prog. Surf. Sci.*, *78*, 1.
[73] Williams, R. & Dresner, J. (1967). *J. Chem. Phys.*, *46*, 2133.
[74] Campbell, I. H. & Smith, L. D. (1999). *Appl. Phys. Lett.*, *74*, 561.
[75] Dresner, J. (1968). *Phys. Rev. Lett.*, *21*, 356 and references therein.
[76] Perluzzo, G., Bader, G., Caron, L. G., & Sanche, L. (1985). *Phys. Rev. Lett.*, *55*, 545.
[77] Ueno, N., Sugita, K., Seki, K., & Inokuchi, H. (1986). *Phys. Rev.*, *B34*, 6386.
[78] Ueno, N., Sugita, K., Seki, K., & Inokuchi, H. (1985). *Jpn. J. Appl. Phys.*, *24*, 1156.
[79] Himpsel, F. J. (1990). *Surf. Sci. Rep.*, *12*, 1.
[80] Frank, K. H., Dudde, R., & Koch, E.-E. (1986). *Chem. Phys. Lett.*, *132*, 83.
[81] Frank, K. H., Yannoulis, P., Dudde, R., & Koch, E.-E. (1988). *J. Chem. Phys.*, *89*, 7569.
[82] Meyer III, H. M., Wagener, T. J., Weaver, J. H., Feyereisen, M., & Almloef, J. (1989). *Chem. Phys. Lett.*, *164*, 527.
[83] Weaver, J. H., Martins, J. L., Komeda, T., Chen, Y., Troullier, N., Ohno, T. R., Kroll, G. H., Haufler, R. E., & Smalley, R. E. (1991). *Phys. Rev. Lett.*, *66*, 1741.
[84] Wu, C. I., Hirose, Y., Sirringhaus, H., & Kahn, A. (1997). *Chem. Phys. Lett.*, *272*, 43.
[85] Hill, I. G., Kahn, A., Cornill, J., dos Santos, D. A., & Bredas, J. L. (2000). *Chem. Phys. Lett.*, *317*, 444.
[86] Sato, N., Yoshida, H., & Tsutsumi, K. (2000). *J. Mater. Chem.*, *10*, 85.
[87] Dutton, G. & Zhu, X.-Y. (2001). *J. Phys. Chem.*, *B105*, 10912.
[88] Ino, D., Watanabe, K., Takagi, N., & Matsumoto, Y. (2003). *Chem. Phys. Lett.*, *383*, 261.
[89] Song, J. K., Han, S. Y., Chu, I., Kim, J. H., Kim, S. K., Lyapustina, S. A., Xu, S., Nilles, J. M., & Bowen, Jr., K. H. (2002). *J. Chem. Phys.*, *116*, 4477.

[90] Oji, H., Mitsumoto, R., Ito, E., Ishii, H., Ouchi, Y., Seki, K., Yokoyama, T., Ohta, T., & Kosugi, N. (1998). *J. Chem. Phys.*, *109*, 10409.
[91] Agren, H., Vahtras, O., & Caratetta, V. (1995). *Chem. Phys.*, *196*, 47.
[92] Mele, E. J. & Ritsko, J. J. (1979). *Phys. Rev. Lett.*, *43*, 68.
[93] Bruehwiller, P. A., Maxwell, A. J., Puglia, C., Nilsson, A., Andersson, S., & Martensson, M. (1995). *Phys. Rev. Lett.*, *74*, 614.
[94] Narioka, S., Ishii, H., Ouchi, Y., Yokoyama, T., Ohta, T., & Seki, K. (1995). *J. Phys. Chem.*, *99*, 1332.
[95] Gordon, M. L., Tulumello, D., Cooper, G., Hitchcock, A. P., Glatzel, P., Mullins, O. C., Cramer, S. P., & Bergmann, U. (2003). *J. Phys. Chem.*, *A107*, 8512.
[96] Huefner, S. (2003). *Photoelectron Spectroscopy: Principles and Applications*, 3rd Ed. Springer: Berlin.
[97] Ishii, H. & Seki, K. (1997). *IEEE Trans. Electron Devices*, *44*, 1295.
[98] Woodruff, T. A., Delchar, D. R., Clarke, S., & Suresh, I. M. (1994). *Modern Techniques of Surface Science*, 2nd Ed., Cambridge University Press: Cambridge.
[99] Campbell, I. R., Rubin, S., Zawodzinski, T. A., Kress, J. D., Martin, R. L., Smith, D. L., Narashkov, N. N., & Ferraris, J. P. (1996). *Phys. Rev.*, *B54*, R14321.
[100] Kotani, M. & Akamatu, H. (1970). *Bull. Chem. Soc. Jpn.*, *43*, 30.
[101] Kotani, M. & Akamatu, H. (1971). *Disc. Faraday Soc.*, *51*, 94.
[102] Hiramoto, M., Ihara, K., & Yokoyama, M. (1995). *Jpn. J. Appl. Phys.*, *34*, 3803.
[103] Pfeiffer, M., Leo, K., & Karl, N. (1996). *J. Appl. Phys.*, *80*, 6880.
[104] Hayashi, N., Ishii, H., Ouchi, Y., & Seki, K. (2002). *J. Appl. Phys.*, *92*, 3784.
[105] Ishii, H., Hayashi, N., Ito, E., Washizu, Y., Sugi, K., Kimura, Y., Niwano, M., Ouchi, Y., & Seki, K. (2004). *Phys. Stat. Sol.*, *(a)201*, 1075.
[106] Chen, C., Gao, W., & Kahn, A. (2004). *J. Vac. Sci. Tech.*, *A22*, 1488.
[107] Ishii, H. & Seki, K. (2002). In: *Conjugated Polymer & Molecular Interfaces: Science & Technology for Photonic & Optoelectronic Applications*, Salaneck, W. R., Seki, K., Kahn, A., & Pireaux, J.-J. (Eds.), Chapter 10, Marcel Dekker: New York, 293.
[108] Hayashi, N., Ito, E., Ishii, H., Ouchi, Y., & Seki, K. (2001). *Synth. Meals*, *121*, 1717.
[109] Munakata, T., Sugiyama, T., Masuda, T., Aida, M., & Ueno, N. (2004). *Appl. Phys. Lett.*, *85*, 3584.
[110] Rotermund, H., Engel, W., Jakubith, S., von Oertzen, A., & Ertl, G. (1991). *Ultramicroscopy*, *36*, 164.
[111] Müller, K., Burkov, Y., & Schmeisser, D. (2006). *Thin Solid Films*, *495*, 219.
[112] Johansson, M. K.-J., Maxwell, A. J., Gray, S. M., Brühwiler, P. A., Mancini, D. C., Johansson, L. S. O., & Mårtensson, N. (1996). *Phys. Rev*., B*54*, 13472.
[113] Maltezopoulos, T., Kubetzka, A., Morgenstern, M., Wiesendanger, R., Lemay, S. G., & Dekker, C. (2003). *Appl. Phys. Lett.*, *83*, 1011.
[114] Lindsay, S. M. (2006). *Faraday Discussions*, *131*, 403.
[115] Hauschild, A., Karki, K., Cowie, B. C. C., Rohlfing, M., Tautz, F. S., & Sokolowski, M. (2005). *Phys. Rev. Lett.*, *94*, 036106.
[116] Ludwig, C., Gompf, B., Petersen, J., Strohmaier, R., & Eisenmenger, W. (1994). *Z. Phys.*, *B93*, 365.
[117] Nonnenmacher, M., O'Boyle, M. P., & Wickramasinghe, H. K. (1991). *Appl. Phys. Lett.*, *58*, 2921.
[118] Fujihira, M. (1999). *Ann. Rev. Mat. Sci.*, *29*, 353.
[119] Umeda, K., Kobayashi, K., Ishida, K., Hotta, S., Yamada, H., & Matsushige, K. (2001). *Jpn. J. Appl. Phys.*, *40*, Part 1, 4381.
[120] Nakamura, M., Goto, N., Ohashi, N., Sakai, M., & Kudo, K. (2005). *Appl. Phys. Lett.*, *86*, 122112.

[121] Fowell, A. E., Williams, R. H., Richardson, B. E., Cafolla, A. A., Westwood, D. I., & Woolf, D. A. (1991). *J. Vac. Sci. Tech.*, *B9*, 581.
[122] Li, W., Kavanagh, K. L., Matzke, C. M., Talin, A. A., Léonard, F., Faleev, S., & Hsu, J. W. P. (2005). *J. Phys. Chem.*, *B109*, 6252.
[123] Troadec, C., Kunardi, L., & Chandrasekhar, N. (2005). *Appl. Phys. Lett.*, *86*, 072101.
[124] Seki, K. (1989). In: *Optical Techniques to Characterize Polymer Systems*, Bässler, H. (Ed.), Elsevier: Amsterdam, 115–180.
[125] Salaneck, W. R., Stafström, S., & Bredas, J. L. (1996). *Conjugated Polymer Surfaces and Interfaces*, Cambridge University Press: Cambidge.
[126] Löglund, M., Greczynski, G., Crispin, A., Fahlman, M., Salaneck, W. R., & Kugler, T. (2002). In: *Conjugated Polymer & Molecular Interfaces: Science & Technology for Photonic & Optoelectronic Applications*, Salaneck, W. R., Seki, K., Kahn, A., & Pireaux, J.-J. (Eds.), Marcel Dekker: New York, 73–112.
[127] Shen, C., Kahn, A., & Hill, I. (2002). In: *Conjugated Polymer & Molecular Interfaces: Science & Technology for Photonic & Optoelectronic Applications*, Salaneck, W. R., Seki, K., Kahn, A., & Pireaux, J.-J. (Eds.), Marcel Dekker: New York, 351–400.